Tetrahydrobiopterin Binding to Aromatic Amino Acid Hydroxylases. Ligand Recognition and Specificity

Knut Teigen,[†,#] Khanh K. Dao,[†,#] Jeffrey A. McKinney,[†] Antonius C. F. Gorren,[‡] Bernd Mayer,[‡] Nils Åge Frøystein,[§] Jan Haavik,[†] and Aurora Martínez*[,†]

Department of Biomedicine, University of Bergen, Jonas Lies vei 91, 5009-Bergen, Norway, Department of Pharmacology and Toxicology, Karl-Franzens-University, Graz, Austria, and Department of Chemistry, University of Bergen, Allégaten 41, N-5007 Bergen, Norway

Received March 26, 2004

The three aromatic amino acid hydroxylases (phenylalanine, tyrosine, and tryptophan hydroxylase) and nitric oxide synthase (NOS) all utilize (6*R*)-L-*erythro*-5,6,7,8-tetrahydrobiopterin (BH_4) as cofactor. The pterin binding site in the three hydroxylases is well conserved and different from the binding site in NOS. The structures of phenylalanine hydroxylase (PAH) and of NOS in complex with BH_4 are still the only crystal structures available for the reduced cofactor−enzyme complexes. We have studied the enzyme-bound and free conformations of BH_4 by NMR spectroscopy and molecular docking into the active site of the three hydroxylases, using endothelial NOS as a comparative probe. We have found that the dihydroxypropyl side chain of BH_4 adopts different conformations depending on which hydroxylase it interacts with. All the bound conformations are different from that of BH_4 free in solution at neutral pH. The different bound conformations appear to result from specific interactions with nonconserved amino acids at the BH_4 binding sites of the hydroxylases, notably the stretch 248−251 (numeration in PAH) and the residue corresponding to Ala322 in PAH, i.e., Ser in TH and Ala in TPH. On the basis of analysis of molecular interaction fields, we discuss the selectivity determinants for each hydroxylase and explain the high-affinity inhibitory effect of 7-tetrahydrobiopterin specifically for PAH.

Introduction

The aromatic amino acid hydroxylases, including phenylalanine hydroxylase (PAH), tyrosine hydroxylase (TH), and tryptophan hydroxylase (TPH) are important non-heme-iron enzymes involved in the catabolism of L-phenylalanine, the synthesis of catecholamines, and the synthesis of serotonin, respectively, using tetrahydrobiopterin (BH_4) as natural cofactor.[1] BH_4 contains a condensed pyrimidopyrazine ring system with three chiral centers at C6, C1′, and C2′, and the configuration found in mammals is almost exclusively (6*R*,1′*R*,2′*S*)-6-(1′,2′-dihydroxypropyl)-5,6,7,8-tetrahydrobiopterin.[2] PAH, TH, and TPH incorporate one atom of dioxygen into the aromatic substrate[1] and the other in position C4a of the pterin cofactor, forming a pterin-4a-carbinolamine, which is converted to quinonoid dihydrobiopterin (q-BH_2) by pterin-4a-carbinolamine dehydratase. q-BH_2 is regenerated immediately to BH_4 by a NADPH-linked reaction catalyzed by dihydropteridine reductase. Consequently, defects in either the regenerating or the de novo biosynthetic pathways of BH_4 from GTP can lead to metabolic disorders characterized by hyperphenylalaninemia and diminished dopamine and serotonin synthesis.[3] The aromatic amino acid hydroxylases are structurally and functionally similar, and the mammalian forms include a regulatory N-terminal domain, a catalytic domain (sharing more than 80% sequence identity) (Figure 1), and a C-terminal oligomerization domain.[1] This enzyme family thus constitutes an important test system for the study of specific enzyme-bound ligand (BH_4) conformations and selectivity determinants. Recent structural analyses with the oxidized cofactor analogue BH_2[4−7] and with BH_4[8,9] have provided information on the binding motifs in the hydroxylases. The pterin stacks with a phenylalanine residue (Phe254 in PAH) and the N3 and the amino group at the C2 hydrogen bond with the carboxylic group of a conserved glutamic residue (Glu286 in PAH). In the crystal structure of the binary complexes in the absence of substrate or substrate analogue, these hydrogen bonds are water-mediated.[5,8] BH_4 also binds to nitric oxide synthase (NOS), where it functions as a redox-active cofactor and an allosteric effector.[10,11] Different crystal structures have provided insights into the structural basis for the recognition of the cofactor by NOS.[12] There are no conserved residues at the BH_4 binding site between NOS and the aromatic amino acid hydroxylases, but the presence of aromatic amino acids stacking with the pterin ring is a conserved theme, as is the carboxylate (from the propionate heme in the case of NOS) interaction with the amino group at N3 of BH_4.[11]

PAH, TH, and TPH show a comparable affinity for BH_4 and a broad specificity with respect to the size and polarity of the substitutions at the C6 position of the pterin[13] where it has been shown that a number of alkoxymethyl substituents do not impede activity, while substitutions at C2, C4, N5, and N8 abolish the cofactor activity of the analogues.[14,15] All three hydroxylases are potential targets for developing selective cofactor ana-

* To whom correspondence should be addressed. Phone: (47)-55586427. Fax: (47)55586360. E-mail: aurora.martinez@biomed.uib.no.
† Department of Biomedicine, University of Bergen.
# These authors contributed equally to this work.
‡ Karl-Franzens-University Graz.
§ Department of Chemistry, University of Bergen.

10.1021/jm0497646 CCC: $27.50
Published on Web 10/15/2004

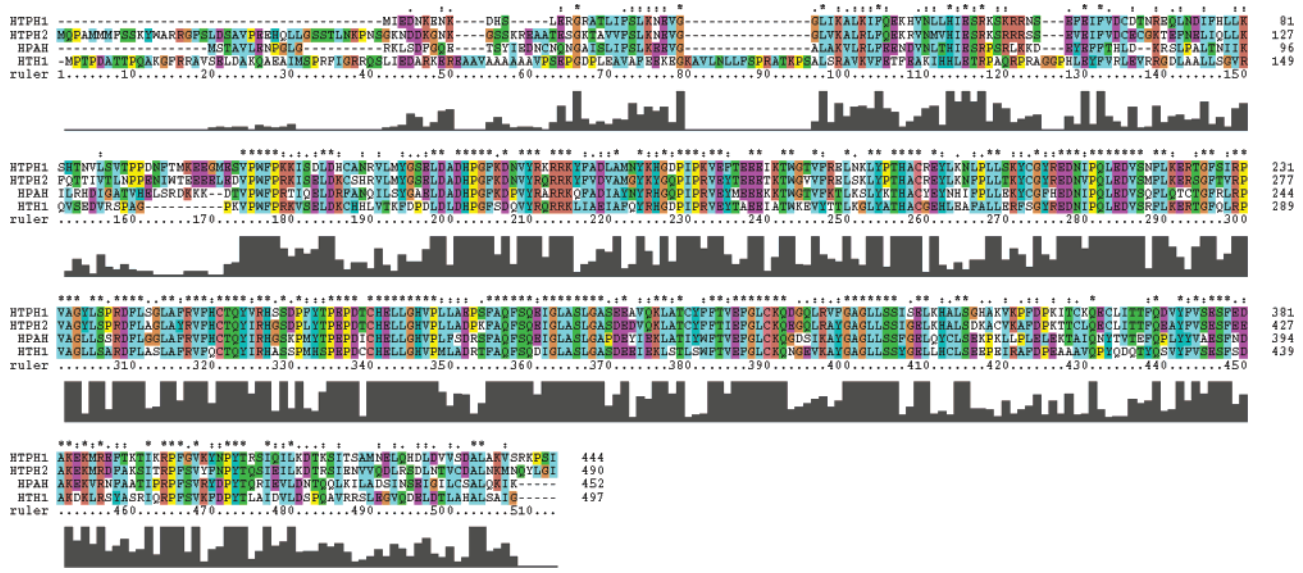

Figure 1. Sequence alignment of human TPH1 (SWISS-PROT P17752), human TPH2 (TrEMBL Q8IWU9), human PAH (SWISS-PROT P00439), and human TH1 (SWISS-PROT P07101). The asterisks above and the highest bars below the sequences indicate identity, while homologue properties of the residues are indicated with two dots or one dot and by the relative height of the columns, depending on the degree of similarity. The two TPH forms found in mammals, TPH1 and TPH2, appear to be mainly expressed in the gut and the brain, respectively.[36] In humans, PAH is mainly expressed in liver and kidney, and TH is found in dopaminergic and noradrenergic neurons in the brain, in the peripheral sympathetic nervous system, and in the adrenal medulla.

logues that can specifically increase the activity of each hydroxylase, i.e., PAH in BH_4 responsive phenylketonuria,[16,17] TH in Parkinson's disease,[18] and TPH in diverse neuropsychiatric syndromes with impaired serotonin biosynthesis.[19] In order to keep the correct redox potential and catalytic function of the cofactor analogues, the acceptable substitutions appear to be limited to the C6 and C7 position.[15] However, also substitutions at these two positions may be problematic because they may result in uncoupled reactions of the aromatic amino acid hydroxylases, with a higher ratio of cofactor oxidation per amino acid substrate hydroxylation and concomitant production of reactive oxygen species.[13] Thus, while oxidation of the cofactor BH_4 is tightly coupled to formation of hydroxylated substrate, the use of alternative cofactor analogues often results in uncoupling of the reaction.[13,15] Therefore, the preparation of BH_4 analogues with an inhibitory effect seems to be a more convenient approach to obtain target specificity.

TPH is highly expressed in serotonin-producing tumors such as small cell lung carcinomas and carcinoids.[20] An inactive cofactor analogue or a suicide inhibitor specific for TPH could thus be used as a chemotherapeutic agent against these tumors. Specific inhibitors for PAH are useful in the preparation of phenylketonuric model animals, since the currently used drug, *p*-chlorophenylalanine, also inhibits TPH with comparable affinity.[21,22]

Here, we present an NMR and molecular docking study of BH_4 binding to the catalytic domains of human PAH,[23] rat TH,[24] human TPH1,[5] and the oxygenase domain of bovine eNOS.[25] The combined use of interatomic distance restraints from NMR and computational structural biology methods using the crystal structures results in reliable conformations of enzyme-bound BH_4, showing a distinct binding mode of the 1,2-dihydroxypropyl side chain at C6 to each of the hydroxylases. The specific bound conformations of BH_4 may be used to propose new functional groups on the pterin moiety that could give rise to pterin analogues capable of discriminating between the different target enzymes under study. Throughout the work we have used recombinant endothelial NOS (eNOS) as a comparative structural probe because active cofactor analogues for the hydroxylases with the moiety 4-oxo intact are potential inhibitors for the NOS isoforms.[26,27]

Results

Conformation of Free BH_4 in Solution at Neutral pH. We first investigated the structure of BH_4 in solution at neutral pH. Dithiothreitol (DTT) addition ensured that both free and enzyme-bound BH_4 (see below) were stable at neutral pH for extended time periods (up to 48 h at 20 °C).[28] Resonance assignments of ^1H signals of BH_4 were obtained from DQF-COSY (not shown) and NOESY (Figure 2) experiments performed at pH 6.0−7.0. Because of the puckered conformation of the pterin ring,[2,8] the H7proS and H7proR signals of BH_4 are resolvable by NMR spectroscopy. A complete assignment of proton resonances in free BH_4 at neutral pH has previously been performed by Bracher et al.[29] and was corroborated in this study. Strong cross relaxation between the methyl protons and H2′, H1′, and H6, respectively, and of H6 with H2′ and H1′, respectively (Figure 2), indicated a conformation of BH_4 in solution with the dihydroxypropyl side chain at C6 curling toward the pyrazine ring. From the 30 structures generated by DGII using the experimental distance restraints from NMR and the chiral and prochiral restrictions, 27 conformers were found to be in agreement with all the restraints and did not present any covalent geometry violation. The conformers could be grouped in two families, one consisting of 19 structures with axial configuration of the side chain relative to the pterin ring (rmsd of 0.35 Å for all atoms) and another one with 8 structures with equatorial configuration (rmsd of 0.29

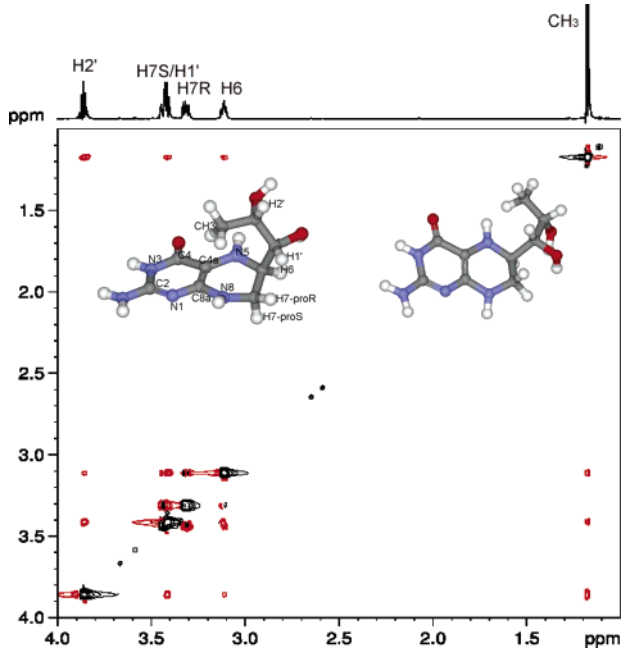

Figure 2. Solution conformation of free BH_4: expanded region of the NOESY spectrum of BH_4 (5 mM) without enzyme (1 s mixing time, in 100 mM K-phosphate, 200 mM KCl, pH 6.7, 10 mM deuterated DTT, 10% D_2O at 293 K). Cross-peaks of opposite sign with respect to the diagonal are shown in red. The NMR-based and distance geometry (DGII) based conformations of free BH_4 are also shown with axial (left) and equatorial (right) configurations of the side chain at C6 and cis configuration of the hydroxyls.

Å) (representative structures of each family are shown in Figure 2). Both families show an almost-cis configuration of the H1′ and H2′ protons (Table 1), which is consistent with the strong cross-peak observed between these protons in the NOESY spectra. The axial and equatorial conformers of BH_4 in solution may in fact represent real solution conformations due to the conformational flexibility of the cofactor and are in agreement with the results obtained by molecular dynamics (MD) simulations.[30,31] In addition, measurements of the $^3J_{HH}$ in free BH_4 for the H6−H7proS (3.2−3.3 Hz) and H6−H7proR (7.5−8.8 Hz) proton pairs are also indicative of an average conformation between equatorial and axial configuration of the side chain.[29]

The Enzyme−BH_4 Complexes Studied by NMR. Transferred NOESY (TRNOESY) spectra of BH_4 in the presence of recombinant human PAH, human TH (isoform 1, TH1), the stable catalytic domain of human TPH1 (Δ90TPH), or eNOS present positive cross-peaks, reflecting negative transfer NOEs typical of ligands bound to large macromolecules at favorable exchange conditions (Figure 3). Some qualitative differences exist between the TRNOESY spectra. In particular, only TH1-bound BH_4 showed a cross-peak between the methyl protons of the dihydroxypropyl at C6 and H6, which was very weak (Figure 3B). And while PAH- and TH1-bound BH_4 showed a cross-peak between the methyl protons and the H1′, in TPH1-bound BH_4 the methyl protons only provide cross-peaks with H2′ (Figure 3A−C), indicating different configurations of the side chain. The conformation of BH_4 bound to the three hydroxylases still revealed the cis to *almost cis* configuration of the H1′−H2′ protons, as found in free BH_4, but the torsion angles [OH− C1′−C2′−OH] adopt different values in each enzyme, indicating different bound conformations of the cofactor. A complete change to the trans configuration of the hydroxyls was obtained for eNOS-bound BH_4. The interproton distances estimated from the cross-peak intensity in TRNOESY spectra taken at mixing times ranging from 10 to 50 ms are summarized in Table 1. Preliminary control experiments with iron-free apoenzymes indicated that distances obtained from the build-up curves for cross-peak intensities were not significantly affected by the presence of the metal. The specific exchange rate requirements for allowing TRNOESY cross-peaks to be interpreted in terms of enzyme-bound ligand conformations[32,33] are fulfilled for the enzyme−BH_4 systems. However, even though our distance estimates at least contribute to a consistent picture of the bound BH_4 conformation, we cannot rule out the possibility for $^1H-^1H$ spin diffusion effects for some cross-peaks. Consequently, because of the small number of proton pairs and the approximate character of the distances measured by TRNOESY, the number and the stringency of the restraints used in the DGII procedure were not very high. Various ensembles or families of conformers of BH_4 bound to each hydroxylase were thus obtained as solutions from the NMR-based DGII calculations. We therefore initiated a computational docking procedure in order to aid in the elucidation of the BH_4−enzyme complexes.

Docking of BH_4. The energy-minimized conformer of BH_4 was docked into the crystal structures of the catalytic domains of human PAH,[23] rat TH,[24] human TPH1,[5] and the oxygenase domain of bovine eNOS[25] using DOCK 4.0. Rat TH and human TH1 reveal 93% sequence identity at the catalytic domain. TPH1 and TPH2 also show a very high sequence identity (about 83%) at the catalytic domains (Figure 1), and the rmsd for backbone atoms between the modeled structure of the catalytic domain of TPH2 (residues 150−490) and the crystal structure of the corresponding region of TPH1[5] was 0.25 Å. This close sequence and structural similarity most probably warrant that the conclusions inferred from docking with human TPH1 hold for human TPH2 as well. During the docking procedure, full flexibility of the ligand was allowed while the proteins were kept rigid. For each enzyme-bound BH_4, the resulting top-scoring docked conformer was subjected to energy minimization and MD simulation, allowing flexibility in the docked ligand and in the side chains from amino acids with an atom within a 5 Å radius from the pterin. The resulting complexes in which flexibility was allowed are shown in Figure 4 for PAH·BH_4, TH·BH_4, TPH1·BH_4, and eNOS·BH_4, respectively. The interproton intramolecular distances measured on the top-scoring docked conformers after MD simulations agreed roughly with the NMR restraints (Table 1), and the docked BH_4 structures were present among the ensembles obtained by the NMR-based DGII calculations (data not shown).

Analysis of the BH_4 bound and unbound crystal structures of PAH shows that binding induces a small conformational change of the enzyme (induced fit) involving residues Leu248, Leu255, Gly27, as well as of the side chain of BH_4.[8] Also, binding of BH_4 to eNOS

Table 1. Interproton Distances (Å) from the Observable Protons of BH_4, As Estimated from NOESY Spectra (Free BH_4) and TRNOESY Spectra (Enzyme-Bound BH_4)[a]

proton pair	free BH_4 (axial/equatorial)	enzyme-bound BH_4			
		PAH·BH_4	TH·BH_4	TPH1·BH_4	eNOS·BH_4
CH3−H2′ [b]	2.5[c]	2.5[c]	2.5[c]	2.5[c]	2.5[c]
CH3−H1′ [b]	i (3.2/3.0)	i (3.0)	l (3.6)	Nc[d] (3.8)	Nc[d] (2.9)
CH3−H6[b]	i (4.0/3.3)	Nc[d] (3.5)	l (3.2)	Nc[d] (3.3)	Nc[d] (4.5)
CH3−H7proR[a]	Nc[d] (5.0/4.6)	Nc[d] (4.4)	Nc[d] (5.2)	Nc[d] (5.1)	Nc[d] (4.8)
H1′−H2′	vs (2.4/2.5)	vs (2.4)	vs (2.5)	s (2.6)	i (3.1)
H6−H7proR	s (2.7/3.1)	s (3.1)	s (3.1)	s (3.1)	s (3.0)

[a] In parentheses, distances (in Å) as measured in the structure with the lowest rmsd with respect to the ensembles after DGII for free BH_4 (axial and equatorial conformations) and in the top-scoring docked structures after molecular dynamics simulations for enzyme-bound BH_4. Interproton distances: vs, very short distance (<2.5 Å); s, short distance (2.5−3.0 Å); i, intermediate distance, (3.1−3.5 Å); l, long distance (>3.5 Å). [b] Center averaging was employed between the protons, and the appropriate corrections were added to the upper distance limit.[49] [c] Internal standard. [d] Nc: no cross-peak observed.

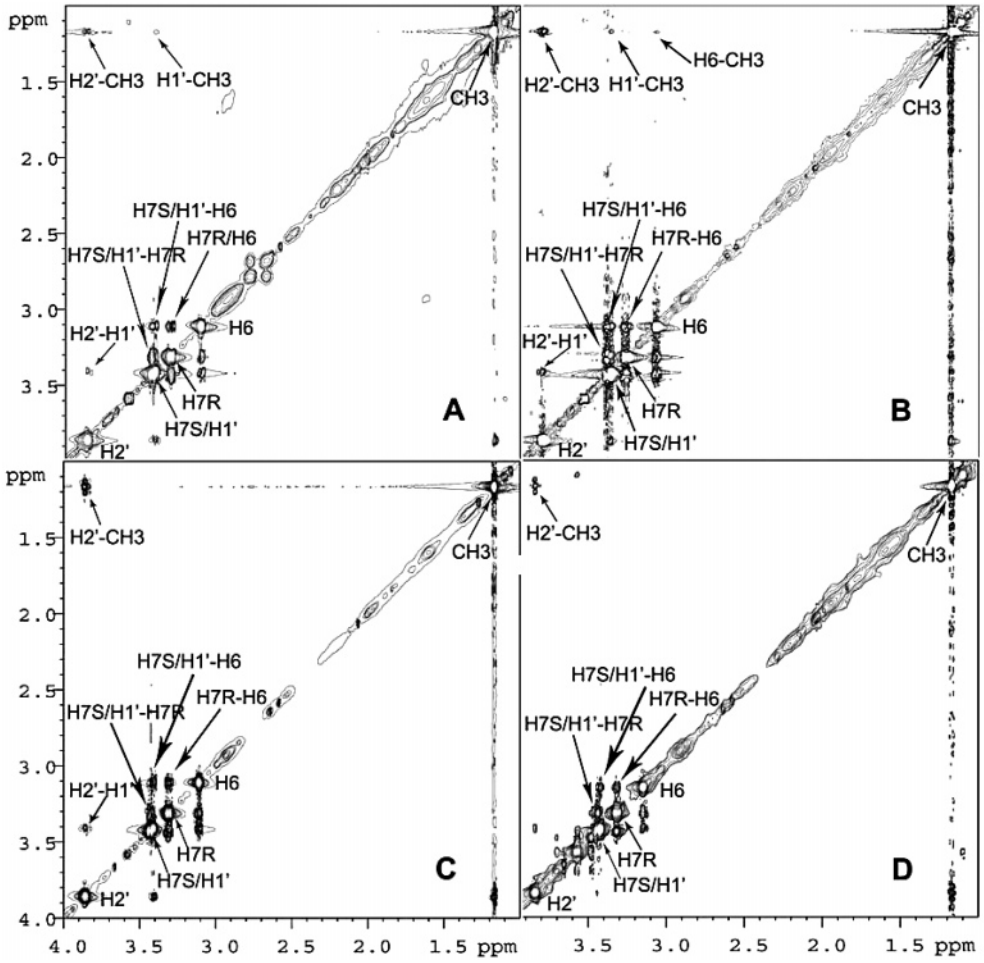

Figure 3. TRNOESY spectra of BH_4 (5 mM) in the presence of enzyme showing cross-peaks of the same sign as the diagonal: (A) human PAH, 0.12 mM subunit, pH 6.0, 90 ms mixing time; (B) human TH1, 0.12 mM subunit, pH 6.7, 100 ms mixing time; (C) human Δ90TPH1, 0.12 mM subunit, pH 6.7, 100 ms mixing time; (D) bovine eNOS, 0.10 mM subunit, pH 6.2, 100 ms mixing time. All spectra were obtained in the presence of 10 mM deuterated DTT, 100 mM K-phosphate, 200 mM KCl, and 10% D_2O at 293 K.

seems to be accompanied by minor changes in protein backbone, apart from a reorientation of the indole ring of Trp449 and of the propionates of the heme.[25] Our docking procedure complemented with short MD simulations would certainly not completely mimic the final structure of the binary complex. Nevertheless, in the case of the complexes PAH·BH_4 and eNOS·BH_4, for which crystal structures are available[8,9,25] (shown in parts A and D of Figure 4 (insets) for comparison), there was good agreement between complexes obtained from crystallography and docking, as shown among others by the dihedral angle [OH−C1′−C2′−OH] and rmsd analysis. Specifically, the dihedral angle was 51.2° in the docked structure of the PAH·BH_4 complex and 60.8° and 63.4° in the binary[8] and ternary[9] X-ray structures of the complexes of the cofactor with PAH, respectively. The value of this angle in the docked structure for the complex of BH_4 with eNOS was 162.1° versus 178.4° in the crystal structure.[25] The rmsd between the docked structure compared with the binary PAH·BH_4[8] and the ternary PAH·BH_4·L-thienylalanine complexes[9] were 2.0 and 1.8 Å, respectively. However, when the cofactor

Table 2. Pairwise Root Mean Square Distances (rmsd)[a] between BH_4 Heavy Atoms

	X-ray PAH·BH_4 binary[b] (Å)	X-ray PAH·BH_4 tertiary[c] (Å)	docking of free BH_4 to PAH[d] (Å)
X-ray PAH·BH_4 tertiary[c]	0.14		
docking of free BH_4 to PAH[d]	1.39	1.38	
docking of BH_4 to PAH[e]	0.45	0.41	1.25

[a] Alignment performed with Qmol[50] prior to rmsd calculation. [b] The structure of the PAH·BH_4 complex.[8] [c] The structure of the PAH·BH_4·L-thienylalanine complex.[9] [d] This work, no flexibility allowed. [e] This work, ligand flexibility allowed.

molecules are aligned, the rmsd value between BH_4 heavy atoms in the docked and the corresponding X-ray conformer was low, i.e., about 0.41−0.45 Å with the two X-ray complexes of PAH and BH_4 and 0.46 Å with the complex of BH_4 and NOS. Table 2 summarizes the pairwise rmsd for the aligned BH_4 atoms in each PAH·BH_4 complex. Thus, the rearrangement of the side chain of BH_4 and the specific interactions between the cofactor and amino acids in the active site observed in the X-ray structures appear to be properly reproduced in the structures obtained by the docking procedure including flexibility and validated by NMR (Figure 4 and Table 2). Thus, the application of these docked structures to analyze selectivity determinants for cofactor binding appears to be justified. On the other hand, when docking was performed with the fixed conformation obtained by NMR for free BH_4 (with the side chain at C6 either in equatorial or in axial configurations, Figure 2), without allowing full flexibility of the ligand in the docking procedure, poor agreement was obtained between the top-scoring docked structures and the crystallographic structures (see Figure 4A showing the top-scoring PAH·BH_4 complexes obtained by docking without (green) and with (red) flexibility). The two resulting biopterin conformations are flipped 180° with respect to each other. When only flexibility is allowed, the conformer has the O4 atom pointing in the correct direction toward the active site iron, as in the X-ray structure (see inset in Figure 4A and Table 2).

In the mammalian aromatic amino acid hydroxylases, the pterin ring of BH_4 π-stacks with a conserved Phe residue (254 in PAH (Figure 4A), 300 in TH (Figure 4B), 241 in TPH1 (Figure 4C), and 287 in TPH2 (not shown)). The N3 and the amino group at C2 hydrogen-bond with the carboxylic group of a Glu residue (286 in PAH, 332 in TH, 273 in TPH1, and 319 in TPH2) (parts A−C of Figure 4). The pterin ring also establishes specific contacts with other nonconserved (His264(PAH)/Gln310(TH)/His251(TPH1)) and conserved (Leu249-(PAH)/Leu295(TH)/Leu236(TPH1)) residues. The dihydroxypropyl side chain is located at a large hydrophobic pocket surrounded by Ser251, Ala322, Trp326, and Tyr325 in PAH, Ala297, Ser368, Trp372, and Tyr371 in rat TH, and in the TPH1·BH_4 complex the methyl group of BH_4 is also in proximity to several hydrophobic and aromatic residues (Tyr312, Phe313, Ala309, Pro238, and Tyr235). In the PAH·BH_4 complex, the hydroxyl group OH2′ hydrogen-bonds with the hydroxyl group of Ser251 (d(O2′−O) = 2.9 Å) (Figure 4A). When docking is performed using the full-length form of PAH including the regulatory domain, the configuration of the side chain and the interaction between OH2′ and Ser251 is maintained.[34] In TH and TPH1, Ser251 corresponds to Ala297 and Pro238, respectively (Figure 1). In TH, OH2′ interacts with the hydroxyl of Ser368 (Figure 4B).

A close view at the pterin binding site of eNOS with the docked BH_4 shows the conserved aromatic π-stacking interaction between the pterin ring and a Trp residue from one subunit (Trp449 in bovine eNOS) and a Phe in the other subunit (Phe462) (Figure 4D). In addition, the hydrogen-bond network from the pterin N3 and O4 to the heme propionate, from the pterin O4 and N5 to Arg367 at the substrate binding helix, and from the pterin N2 to the carbonyl oxygen of Val451 are observed. The crystal structure of the complex eNOS·BH_4 essentially displays the same interactions.[25]

Molecular Interaction Fields. A close examination of the docked structures allowed the characterization of common motifs as well as specific binding determinants for the cofactor in each enzyme. The BH_4 binding pocket is located at the bottom of the hydrophobic active site opening and is more negatively charged in the three hydroxylases than in eNOS because of the presence of the Glu286 (numeration in PAH) involved in the binding of the guanidinium group of the pyrimidine ring and because of the iron coordinating residue Glu330 (Figure 4). The binding sites also manifest specific differences in charge distribution and solvent accessible surface that might be exploited in the search of specific cofactor analogues for each hydroxylase. In particular, the backbone arrangement of the short stretch of amino acids close to N1 and N8 of the biopterin (Leu248-Leu249-Ser250-Ser251 in PAH) is somewhat different in the three hydroxylases. This sequence corresponds to Leu-Leu-Ser-Ala in TH, while in TPH1 and TPH2 the corresponding sequence is Tyr-Leu-Ser-Pro (see Figures 1 and 4A−C). To accommodate the Tyr and Pro residues in the active site of TPH, the backbone of this stretch has to be arranged in a different manner. The amino group of the Leu236 (Leu249 in PAH) backbone and the carbonyl oxygen of Gly234 (Gly247 in PAH) are more exposed in TPH (Table 3). The molecular interaction fields (MIFs) show that these groups are more prone to establish hydrogen bonding with a hydroxyl probe (see Figure 5A−C). The backbone arrangement in TPH seems to favor an 8-methylbiopterin, which would be an inhibitory pterin analogue[15] that would not fit as well in the other hydroxylases or NOS (see Figure 5E−H).

Another site in which there appear to be important differences between the hydroxylases is close to the C7 position of the pterin cofactor. Careful investigation of the active site of PAH reveals a unique serine (Ser251) in proximity to position C7. This amino acid corresponds to an Ala in TH and a Pro in the TPHs. A C7 substituent capable of H-bonding with Ser251 could thus increase the selectivity of pterin binding to PAH. In fact, the MIFs show a strong interaction with the amino and hydroxyl probes at the region between Ser251 and Leu249 (parts A and I of Figure 5). When BH_4 is docked in the active site of PAH, this area is at a distance of 2 Å from the C7 atom (Figure 5I). Similar strong interaction with the polar probes in the vicinity of C7 is not found in the other two hydroxylases or NOS (Figure 5). Interestingly, 7-tetrahydrobiopterin (7-BH_4), a BH_4

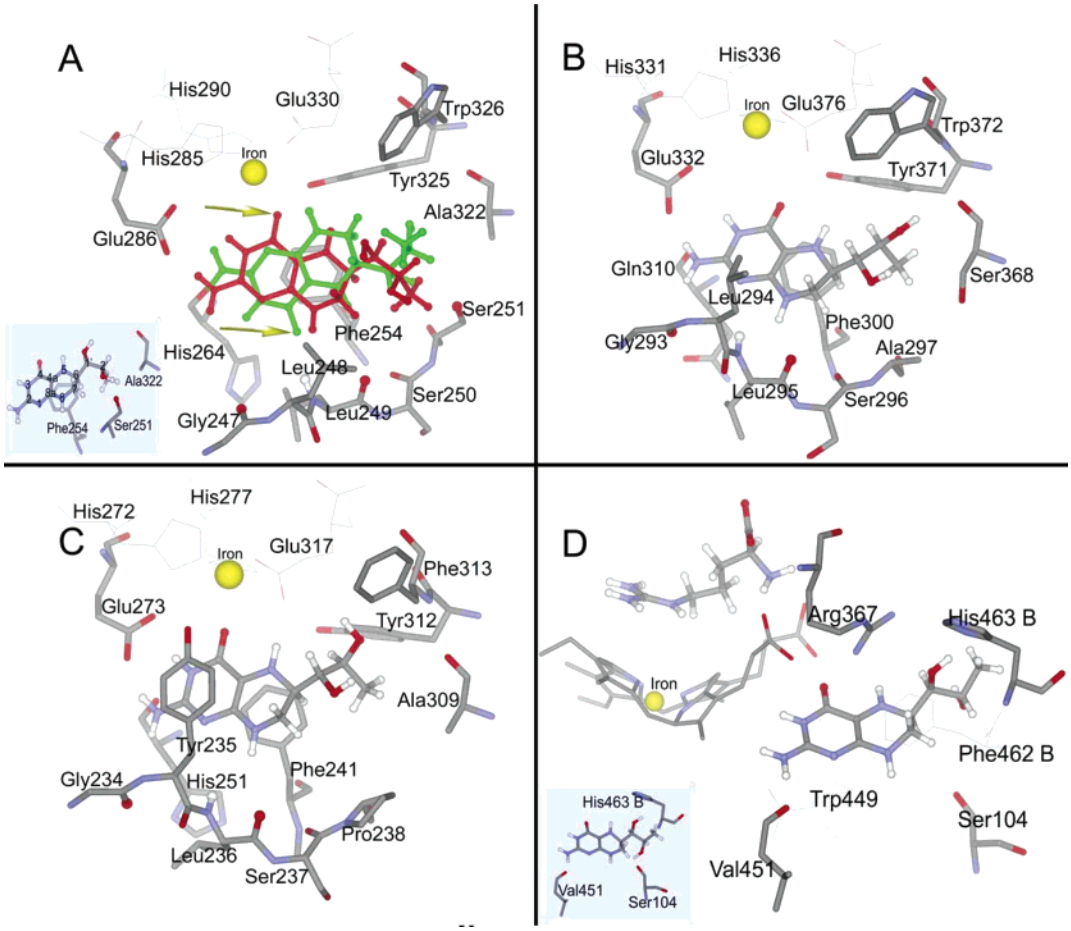

Figure 4. Structure of the enzyme-bound BH_4 for (A) PAH, (B) TH, (C) TPH1, and (D) eNOS. Active site residues at the ligand binding sites are shown as sticks (iron coordinating residues as wires (A−C)) with the oxygen atom in the side chain of Ser251 (A) and the atoms listed in Table 3 (A−C) shown as balls. BH_4 is in ball-and-stick representation, and the iron is in yellow (A−D). The BH_4 structure obtained from docking allowing flexibility of the ligand is shown in red (A) and colored by atom type (B−D). The BH_4 structure colored green (A) shows the binding mode obtained by docking the free BH_4 conformation, and the yellow arrows show the position of the O4 atoms: (A, inset) crystal structure of the PAH·BH_4 complex (PDB code 1J8U); (D, inset) crystal structure of the NOS·BH_4 complex (PDB code 1FOP). The amino acid residues containing the B-letter belong to the second monomer.

Table 3. Surface Accessible Area of Selected Backbone Atoms Calculated by the Program naccess[44] (Numeration of the Amino Acids Refers to PAH)

	in TH (Å^2)	in PAH (Å^2)	in TPH (Å^2)
Gly247 carbonyl oxygen	0.2	0.1	0.9
Leu249 amino nitrogen	0.0	1.0	3.1
Leu249 carbonyl oxygen	2.4	6.7	14.9

analogue with the dihydroxypropyl side chain located at the C7 position, is a strong selective inhibitor of PAH.[35] This inhibitory effect can be explained by a strong interaction of the OH1′ of 7-BH_4 with Ser251/Leu249. The IC_{50} value for the inhibition of this hydroxylase by 7-BH_4 is as low as 1 μM when assays are performed at low physiological (5 μM) concentrations of BH_4 and saturating (1 mM) concentrations of L-Phe. In comparison, the IC_{50} values for TH and TPH are 2500- and 3300-fold higher, respectively.[35] The TPH isoform that was utilized in such a study was isolated from rabbit brain, an isoform that has been recently recognized mainly as TPH2.[36] Using recombinant human PAH, we have now measured an inhibitory constant (K_i(7-BH_4)) of 7 μM and the corresponding value for recombinant human TPH1 was found to be 540-fold higher (3.8 mM).

Discussion

The specific recognition of a protein target showing structural similarity at the binding site with many other proteins is a challenge in pharmacophore elucidation. TRNOESY is a frequently used NMR procedure to determine the specific receptor-bound conformation of ligands, and when combined with molecular docking, it appears to efficiently predict the structure of ligand−protein complexes. Here, we have applied this integrating experimental and computational structural biology methodology to dock a flexible ligand into the crystal structure of three highly homologous and important mammalian enzymes. Subtle differences in the active site pocket give rise to different conformations for the BH_4 when bound to the three aromatic amino acid hydroxylases and allow the analysis of selectivity determinants.

Examination of the BH_4 conformation at neutral pH shows that the hydroxyls at the side chain at C6 appear to adopt a cis configuration in solution, and our results are also compatible with both an equatorial and axial orientation of the side chain at C6.[28] Previous results obtained by MD simulations and measurements of the dihedral angles between the H6 proton and the H7proS

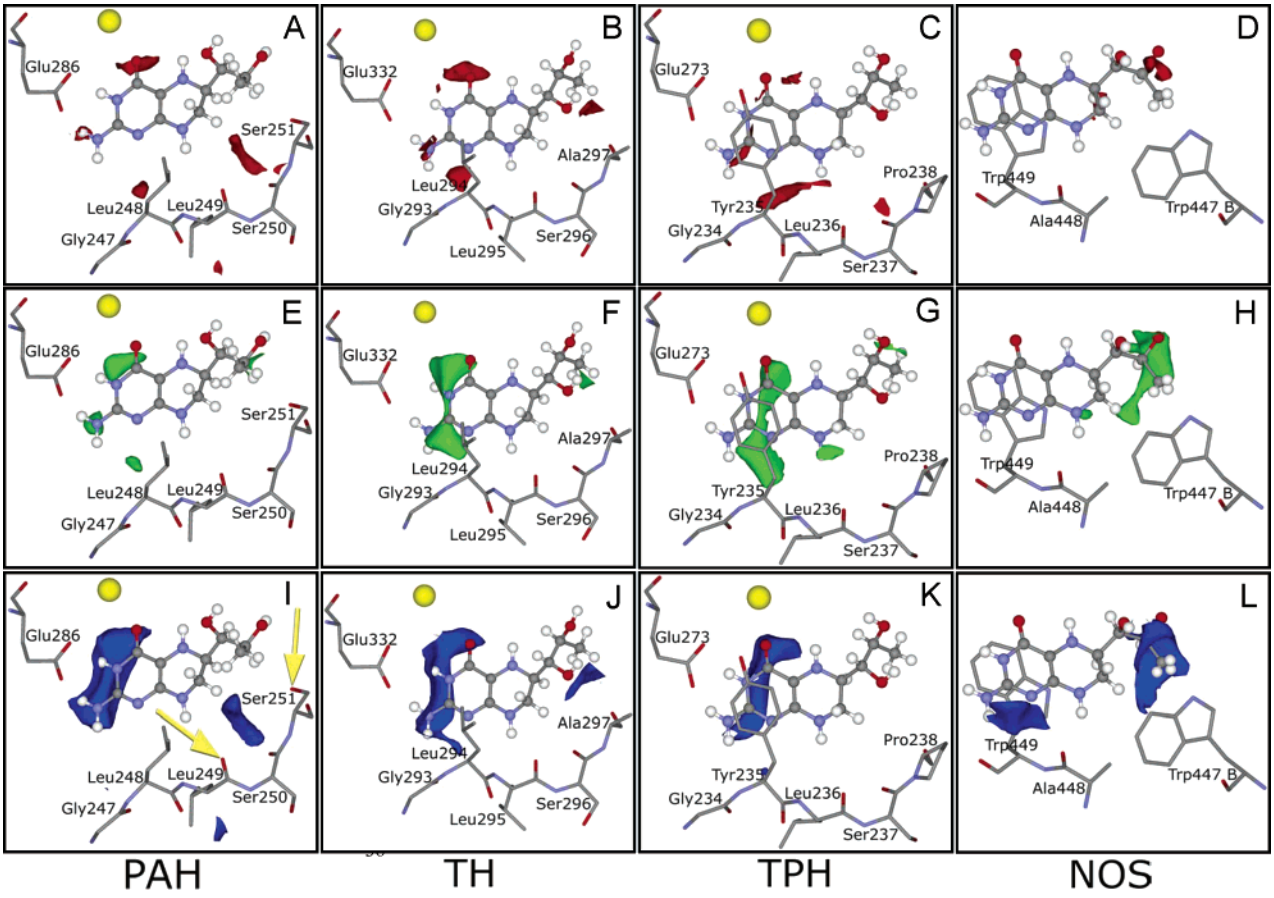

Figure 5. GRID molecular interaction fields (MIFs) for the hydroxyl (red, A−D), methyl (green, E−H), and amino (blue, I−L) probes within the active site pocket of PAH, TH, TPH1, and eNOS, respectively, from left to right. The energy cutoff value is −8.5, −3.5, −9.5 kcal/mol for the hydroxyl, methyl, and amino probes, respectively. Note the yellow arrows in panel I, pointing at the hydroxyl group of Ser251, and the backbone carbonyl oxygen of Leu249 responsible for the strong interaction with both the hydroxyl and amino probe close to C7 of BH_4 bound to PAH.

and H7proR protons by NMR[29,31] have indicated that these two conformers of BH_4 probably coexist in equilibrium at neutral pH. The bioactive bound conformations of BH_4 are, however, compatible with equatorial/pseudoequatorial and more extended conformations for the chain at C6 (Figure 4). For BH_4 bound to PAH and NOS, the crystallographic structures also show equatorial conformations.[8,9,25] Statistical analyses of ligand reorganization upon binding suggest that ligands unfold during binding and tend to bind in a more extended conformation than when free in solution, even if a higher degree of folding is more stable in solution,[37] in agreement with our results with BH_4.

While hydroxylase-bound BH_4 maintains the cis configuration between the H1′ and H2′, our NMR results support a trans configuration of the hydroxyls in BH_4 bound to eNOS. Examination of the eNOS·BH_4 complex[25] (Figure 4D) indicates that the hydrogen bonds between the O1′ and the carbonyl oxygen of Phe462 and between the O2′ and the carbonyl oxygen of Ser104 (Figure 4D) are responsible for the cis to trans conformational change observed from free to NOS-bound BH_4. For BH_4 bound to the aromatic amino acid hydroxylases, the pterin ring always adopts the same binding mode in the active site, interacting with the hydroxylases through π-stacking with an invariant phenylalanine residue (Phe254 in PAH) and a hydrogen-bonding network involving positions 1, 2, 3, 4, 5, and 8 of the pterin ring. In addition to the stacking L-Phe residue, Leu249, Ser250, and Glu286 (in PAH) are also conserved at the pterin binding site in the mammalian hydroxylases. Together with the residues involved in iron binding, i.e., His285, His290, and Glu330 (in PAH), these conserved residues form a *signature sequence for tetrahydrobiopterin binding* to mammalian aromatic amino acid hydroxylases. Specific substitutions in human PAH, TH, or TPH introduce differences in electrostatic potential and shape at the pterin binding sites (Figures 4 and 5) and result in specific interactions and rearrangement of the dihydroxypropyl chain of BH_4. For instance, Leu294 (TH) and Leu248 (PAH) are conserved in all TH and PAH sequences, but it is a larger tyrosine residue in the human TPH1 (Tyr235) and TPH2 (Tyr281) (Figures 1 and 4). In the TPH1·BH_4 complex, the pterin ring is sandwiched between this aromatic residue and Phe241, as also found in the crystal structure of the complex with BH_2.[5] Another important difference at the binding site of the pterin side chain is the corresponding Ala297 (TH), Ser251 (PAH), and Pro238 (TPH1). The specific residues at the active site of TPH1, which are also conserved in TPH2, seem to selectively accommodate pterins with methyl substituents at the N8 position (Figure 5G). 8-Methylbiopterin thus appears as a potential scaffold to further develop TPH-specific inhibitors. In addition to the differences at the pterin binding site, the substitution of Trp326 in PAH and the

corresponding Trp372 in TH by a Phe in both TPH1 and TPH2 allows for the preferential hydroxylation of L-Trp.[7] In the PAH·BH_4 complex the side chain hydroxyl of Ser251 hydrogen-bonds to O2′ (Figure 4A) and this interaction is responsible for the bending of the chain toward the C7 of the pterin ring. The specific residues in PAH at this position seem to be responsible for the high-affinity binding to nearby polar groups and explain the selective high-affinity competitive inhibition by 7-BH_4. In the case of PAH the structure of the regulatory domain has been determined.[38] Molecular modeling studies including MD stimulations have shown that residues from this domain (i.e., Ser23) interact with the dihydroxypropyl side chain.[34] The elucidation of the structures of the N-terminal domains of TH and TPH might aid in the discrimination between the three enzymes and provide additional specificity determinants for the development of cofactor analogues.

In relation to the structure of the NOS·BH_4 complex, the different residues at the pterin binding site between eNOS, the inducible (iNOS), and the neuronal (nNOS) isoforms have prompted the development of iNOS inhibitors with different substituents at C6 of BH_4.[26,27] A similar strategy may be applicable to the development of specific inhibitors for PAH, TH, and TPH. In addition, the selectivity of NOS has to be taken into account when considering potential new cofactors of the aromatic amino acid hydroxylases because 4-oxopteridines with substituents at the C6 position have been found to be effective inhibitors of NOS, while substituents at the C7 position abolish the binding of the cofactor analogues.[26] BH_4 analogues with polar substituents at position 7, such as 7-BH_4, would thus be specific for PAH with respect to the other aromatic amino acid hydroxylases and to NOS isoforms and may be useful in the preparation of phenylketonuric model animals and cells.

Experimental Section

Expression and Purification of the Recombinant Enzymes. All enzymes were obtained by expression in *E. coli* and purified to homogeneity: human PAH,[39] human TH, isoform 1 (TH1),[40] the catalytic domain of human TPH1 (Δ90TPH1),[7] and bovine endothelial NOS (eNOS) oxygenase domain (amino acids 55−491).[10]

Enzyme Activity Assays. PAH activity was assayed with recombinant human PAH at 25 °C[39] and TPH activity with recombinant TPH1 at 30 °C.[7] The inhibitory effect of 7-BH_4 on these hydroxylases was analyzed using various concentrations of 7-BH_4 up to 2 mM and with 25 and 100 μM BH_4 for PAH and 25 and 250 μM BH_4 for TPH, and the reactions were started by the simultaneous addition of the corresponding concentrations of BH_4 and 7-BH_4. The inhibitory constants (K_i) were calculated by nonlinear regression analysis.

Molecular Modeling and Docking. The DOCK 4.0.1 suite of programs (University of California, San Francisco)[41] running on SGI workstations was used to fit the in vacuo energy-minimized conformation of BH_4 into the crystal structures of the catalytic domain of human PAH (residues 143−410) (PDB code 1PAH), rat TH (residues 155−456) (PDB code 1TOH), and human TPH1 in the TPH1·BH_2 complex (PDB code 1MLV) and into the oxygenase domain of bovine eNOS (PDB code 1FOP).[25] Furthermore, the structural model of TPH2[36] was prepared using as template the structure of TPH1 (83% similarity between both TPH isoforms at the 104−393 catalytic region, numeration in TPH1) in the TPH1·BH_2 complex.[5] The model was prepared using the homology modeling capabilities of Swiss-Pdb Viewer in conjunction with SWISS-MODEL.[42] For docking, a grid was constructed for each enzyme with a distance of 20 Å around the Fe^{3+} atom for TH, PAH, and TPH or around the Ne1 atom of Trp447 for eNOS, with a grid spacing of 0.2 Å and a sampling size of 10 000 structures. Water molecules were not included in the preparation of the grids, and the active site iron was treated as a sphere with the correct radius and a charge of +2. Flexibility of the ligand and torsion angle optimization were allowed. The sample structures were scored using the force field energy-based scoring function. Thirty top-scoring structures were analyzed and found to be nearly superimposed and have the anticipated binding mode according to previously published models of enzyme−cofactor complexes.[5−8] A representative model of each of the enzyme−BH_4 complexes obtained from DOCK was subjected to energy minimization and 1 ns MD simulations, allowing flexibility to the BH_4 molecule and to the residues of the enzyme having an atom within 5 Å from the biopterin; the rest of the protein was kept frozen. The complexes were energy-minimized with the AMBER force field by applying a steepest descent minimization followed by a conjugate gradient minimization. Convergence criteria were 10 and 1 kcal/mol, respectively, for the two algorithms. The Discover module of InsightII was used to perform MD simulations with an implicit water model using a distance-dependent dielectric of 4, applying the same restraints as for the minimization procedure. The cutoff radius for nonbonded interactions was 12 Å, with a secondary cutoff radius of 15 Å. The molecular system was allowed to equilibrate to 300 K for 20 ps and then kept at this temperature throughout the 1 ns simulations, with a step length of 1 fs. Coordinates were saved every 1 ps and used to calculate average structures from the simulations. The averaged structures over the last 100 ps of the simulations were energy-minimized as previously described and stored as the final conformation of the enzyme−BH_4 complexes for further analysis.

The programs InsightII (Accelrys), Grid,[43] naccess,[44] and DsViewerPro (Accelrys) were used to analyze the docked structures and to prepare the figures.

NMR Spectroscopy. All NMR samples consisted of 0.5 mL of 5 mM BH_4 with or without enzyme in 100 mM K-phosphate, 200 mM KCl, 10% D_2O, pH 6.7 or the indicated pH, and 10 mM deuterated DTT (C/D/N Isotopes Inc.) to keep BH_4 reduced. The NMR tubes were flushed with argon for 3 min and sealed with an Omni-Fit sample tube valve (Wilmad, Buena, NY). The hydroxylase samples were added to the BH_4 solution at a final protein concentration of ∼0.12 mM subunit. NMR experiments were performed at a probe temperature of 293 K on a Bruker DRX600 NMR spectrometer using a triple resonance 5 mm probe head with inverse (^{1}H) detection and actively shielded triple axis (x,y,z) gradient coils. Acquisition and processing of NOESY spectra of free BH_4 and TRNOESY spectra of enzyme−BH_4 complexes were performed as previously reported, with mixing times of 1 s and 10−50 ms, respectively.[6] Spectral visualization and analysis were carried out on SGI workstations with the program XWINNMR (Bruker). On the basis of K_d values of 2−8 μM for the hydroxylases[45,46] and less than 1 μM for NOS,[47,48] the added enzyme was present solely as a hydroxylase·BH_4 complex at the concentrations of BH_4 (5 mM) and enzyme (0.12 mM subunit) used in the TRNOESY experiments. Interproton distances were estimated from the initial slopes of plots of the cross-peak volume as a function of mixing time,[32] using a distance of 2.5 Å between the average center of CH_3 and the H2′ protons of BH_4 as internal reference. The NMR-based distances restraints, classified in very short (<2.5 Å), short (2.5−3.0 Å), intermediate (3.1−3.5 Å), and long (> 3.5 Å), were used in the distance geometry calculations by DGII (Accelrys).

Molecular Interaction Fields (MIFs). Grid calculations were performed with version 21 of the GRID software[43] on the X-ray structures of the three hydroxylases[5,23,24] and NOS,[25] after removal of the bound ligands. In GRID, selected probes (test molecules and atoms) are moved along the surface of the receptors (the target enzymes) and the theoretical interaction energies are calculated at each point. This procedure generates

the MIFs or maps. The grid interaction box in the receptor structures was chosen to encompass the complete active sites of the enzymes and had a size of 22 Å × 22 Å × 22 Å, with a grid spacing of 0.25 Å. The amino acid side chains were allowed to move (move directive set to 1). Default values have been used for all other directives. From the several chemical probes tested, O1, alkylhydroxy OH group, C3, methyl CH_3 group, and N2, neutral flat NH_2, e.g., amide, provided the most significant differences between the three aromatic amino acid hydroxylases and were further selected for detailed analyses of the interacting regions. The interaction energy was calculated using a force field approach,[43] and the absolute values were stored in a 3D matrix referred to as grid.

Acknowledgment. All members of our laboratories are thanked for technical assistance and critical discussions. This research was supported by grants from the Research Council of Norway and by the Human Frontier Science Program (Grant RGP0026/2001-M).

Appendix

Abbreviations. BH_2, 7,8-erythrodihydrobiopterin; BH_4, (6*R*)-L-*erythro*-5,6,7,8-tetrahydrobiopterin; 7-BH_4, 7-tetrahydrobiopterin; DTT, dithiothreitol; MD, molecular dynamics; MIFs, molecular interaction fields; NOS, nitric oxide synthase; PAH, phenylalanine hydroxylase; rmsd, root-mean-square distance; TH, tyrosine hydroxylase; TH1, human tyrosine hydroxylase isoform 1; TPH, tryptophan hydroxylase; TPH1, human tryptophan hydroxylase isoform 1; TPH2, human tryptophan hydroxylase isoform 2; Δ90TPH1, a truncated form of human tryptophan hydroxylase isoform 1 lacking the N-terminal 90 residues; TRNOESY, transferred nuclear Overhauser effect spectroscopy.

References

(1) Fitzpatrick, P. F. Mechanism of aromatic amino acid hydroxylation. *Biochemistry* **2003**, *42*, 14083−14091.
(2) Matsuura, S.; Sugimoto, T.; Murata, S.; Sugawara, Y.; Iwasaki, H. Stereochemistry of biopterin cofactor and facile methods for the determination of the stereochemistry of a biologically active 5,6,7,8-tetrahydropterin. *J. Biochem.* **1985**, *98*, 1341−1348.
(3) Thöny, B.; Auerbach, G.; Blau, N. Tetrahydrobiopterin biosynthesis, regeneration and functions. *Biochem. J.* **2000**, *347* (Part 1), 1−16.
(4) Erlandsen, H.; Bjørgo, E.; Flatmark, T.; Stevens, R. C. Crystal Structure and Site-Specific Mutagenesis of Pterin-Bound Human Phenylalanine Hydroxylase. *Biochemistry* **2000**, *39*, 2208−2217.
(5) Wang, L.; Erlandsen, H.; Haavik, J.; Knappskog, P. M.; Stevens, R. C. Three-dimensional structure of human tryptophan hydroxylase and its implications for the biosynthesis of the neurotransmitters serotonin and melatonin. *Biochemistry* **2002**, *41*, 12569−12574.
(6) Teigen, K.; Frøystein, N. Å.; Martínez, A. The structural basis of the recognition of phenylalanine and pterin cofactors by phenylalanine hydroxylase: implications for the catalytic mechanism. *J. Mol. Biol.* **1999**, *294*, 807−823.
(7) McKinney, J.; Teigen, K.; Frøystein, N. A.; Salaün, C.; Knappskog, P. M.; et al. Conformation of the substrate and pterin cofactor bound to human tryptophan hydroxylase. Important role of Phe313 in substrate specificity. *Biochemistry* **2001**, *40*, 15591−15601.
(8) Andersen, O. A.; Flatmark, T.; Hough, E. High Resolution Crystal Structures of the Catalytic Domain of Human Phenylalanine Hydroxylase in Its Catalytically Active Fe(II) Form and Binary Complex with Tetrahydrobiopterin. *J. Mol. Biol.* **2001**, *314*, 266−278.
(9) Andersen, O. A.; Flatmark, T.; Hough, E. Crystal Structure of the Ternary Complex of the Catalytic Domain of Human Phenylalanine Hydroxylase with Tetrahydrobiopterin and 3-(2-Thienyl)-L-alanine, and Its Implications for the Mechanism of Catalysis and Substrate Activation. *J. Mol. Biol.* **2002**, *320*, 1095−1108.
(10) Gorren, A. C.; Mayer, B. Tetrahydrobiopterin in nitric oxide synthesis: a novel biological role for pteridines. *Curr. Drug Metab.* **2002**, *3*, 133−157.
(11) Wei, C. C.; Crane, B. R.; Stuehr, D. J. Tetrahydrobiopterin radical enzymology. *Chem. Rev.* **2003**, *103*, 2365−2383.
(12) Crane, B. R.; Arvai, A. S.; Ghosh, D. K.; Wu, C.; Getzoff, E. D.; et al. Structure of nitric oxide synthase oxygenase dimer with pterin and substrate. *Science* **1998**, *279*, 2121−2126.
(13) Kappock, T. J.; Caradonna, J. P. Pterin-Dependent Amino Acid Hydroxylases. *Chem. Rev.* **1996**, *96*, 2659−2756.
(14) Bigham, E. C.; Smith, G. K.; Reinhard, J. F., Jr.; Mallory, W. R.; Nichol, C. A.; et al. Synthetic analogues of tetrahydrobiopterin with cofactor activity for aromatic amino acid hydroxylases. *J. Med. Chem.* **1987**, *30*, 40−45.
(15) Almås, B.; Toska, K.; Teigen, K.; Groehn, V.; Pfleiderer, W.; et al. A Kinetic and Conformational Study on the Interaction of Tetrahydropteridines with Tyrosine Hydroxylase. *Biochemistry* **2000**, *39*, 13676−13686.
(16) Kure, S.; Hou, D. C.; Ohura, T.; Iwamoto, H.; Suzuki, S.; et al. Tetrahydrobiopterin-responsive phenylalanine hydroxylase deficiency. *J. Pediatr.* **1999**, *135*, 375−378.
(17) Matalon, R.; Koch, R.; Michals-Matalon, K.; Moseley, K.; Stevens, R. C. Tetrahydrobiopterin-responsive phenylalanine hydroxylase mutations. *J. Inherited Metab. Dis.* **2003**, *25* (Suppl. 1).
(18) Haavik, J.; Toska, K. Tyrosine hydroxylase and Parkinson's disease. *Mol. Neurobiol.* **1998**, *16*, 285−309.
(19) Martínez, A.; Knappskog, P.; Haavik, J. A structural approach into human tryptophan hydroxylase and its implications for the regulation of serotonin biosynthesis. *Curr. Med. Chem.* **2001**, *8*, 1077−1092.
(20) Walther, D. J.; Peter, J. U.; Bader, M. 7-Hydroxytryptophan, a novel, specific, cytotoxic agent for carcinoids and other serotonin-producing tumors. *Cancer* **2002**, *94*, 3135−3140.
(21) Koe, B. K.; Weissman, A. *p*-Chlorophenylalanine: a specific depletor of brain serotonin. *J. Pharmacol. Exp. Ther.* **1966**, *154*, 499−516.
(22) Chang, N.; Kaufman, S.; Milstien, S. The mechanism of the irreversible inhibition of rat liver phenylalanine hydroxylase due to treatment with *p*-chlorophenylalanine. The lack of effect on turnover of phenylalanine hydroxylase. *J. Biol. Chem.* **1979**, *254*, 2665−2668.
(23) Erlandsen, H.; Fusetti, F.; Martínez, A.; Hough, E.; Flatmark, T.; et al. Crystal structure of the catalytic domain of human phenylalanine hydroxylase reveals the structural basis for phenylketonuria. *Nat. Struct. Biol.* **1997**, *4*, 995−1000.
(24) Goodwill, K. E.; Sabatier, C.; Marks, C.; Raag, R.; Fitzpatrick, P. F.; et al. Crystal structure of tyrosine hydroxylase at 2.3 Å and its implications for inherited neurodegenerative diseases. *Nat. Struct. Biol.* **1997**, *4*, 578−585.
(25) Li, H.; Raman, C. S.; Martasek, P.; Masters, B. S.; Poulos, T. L. Crystallographic studies on endothelial nitric oxide synthase complexed with nitric oxide and mechanism-based inhibitors. *Biochemistry* **2001**, *40*, 5399−5406.
(26) Kotsonis, P.; Frohlich, L. G.; Raman, C. S.; Li, H.; Berg, M.; et al. Structural basis for pterin antagonism in nitric-oxide synthase. Development of novel 4-oxo-pteridine antagonists of (6*R*)-5,6,7,8-tetrahydrobiopterin. *J. Biol. Chem.* **2001**, *276*, 49133−49141.
(27) Matter, H.; Kotsonis, P.; Klingler, O.; Strobel, H.; Frohlich, L. G.; et al. Structural requirements for inhibition of the neuronal nitric oxide synthase (NOS-I): 3D-QSAR analysis of 4-oxo- and 4-amino-pteridine-based inhibitors. *J. Med. Chem.* **2002**, *45*, 2923−2941.
(28) Martínez, A.; Dao, K. K.; McKinney, J.; Teigen, K.; Frøystein, N. Å. The conformation of 5,6,7,8-tetrahydrobiopterin and 7,8-dihydrobiopterin in solution: a NMR study. *Pteridines* **2000**, *11*, 32−33.
(29) Bracher, A.; Eisenreich, W.; Schramek, N.; Ritz, H.; Gotze, E.; et al. Biosynthesis of pteridines. NMR studies on the reaction mechanisms of GTP cyclohydrolase I, pyruvoyltetrahydropterin synthase, and sepiapterin reductase. *J. Biol. Chem.* **1998**, *273*, 28132−28141.
(30) Estelberger, W.; Fuchs, D.; Murr, C.; Wachter, H.; Reibnegger, G. Conformational investigation of the cofactor (6*R*,1′*R*,2′*S*-)-5,6,7,8-tetrahydrobiopterin. *Biochim. Biophys. Acta* **1995**, *1249*, 23−28.
(31) Estelberger, W.; Mlekusch, W.; Reibnegger, G. The conformational flexibility of 5,6,7,8-tetrahydrobiopterin and 5,6,7,8-tetrahydroneopterin: a molecular dynamical simulation. *FEBS Lett* **1995**, *357*, 37−40.
(32) Campbell, A. P.; Sykes, B. D. The two-dimensional transferred nuclear Overhauser effect: theory and practice. *Annu. Rev. Biophys. Biomol. Struct.* **1993**, *22*, 99−122.
(33) Ni, F. Recent developments in transferred NOE methods. *Prog. Nucl. Magn. Reson. Spectrosc.* **1994**, *26*, 517−606.
(34) Teigen, K.; Martínez, A. Probing cofactor specificity in phenylalanine hydroxylase by molecular dynamics simulations. *J. Biomol. Struct. Dyn.* **2003**, *20*, 733−740.
(35) Davis, M. D.; Ribeiro, P.; Tipper, J.; Kaufman, S. "7-Tetrahydrobiopterin," a naturally occurring analogue of tetrahydrobiopterin, is a cofactor for and a potential inhibitor of the aromatic amino acid hydroxylases. *Proc. Natl. Acad. Sci. U.S.A.* **1992**, *89*, 10109−10113.

(36) Walther, D. J.; Peter, J. U.; Bashammakh, S.; Hortnagl, H.; Voits, M.; et al. Synthesis of serotonin by a second tryptophan hydroxylase isoform. *Science* **2003**, *299*, 76.
(37) Perola, E.; Charifson, P. S. Conformational analysis of drug-like molecules bound to proteins: an extensive study of ligand reorganization upon binding. *J. Med. Chem.* **2004**, *47*, 2499−2510.
(38) Kobe, B.; Jennings, I. G.; House, C. M.; Michell, B. J.; Goodwill, K. E.; et al. Structural basis of autoregulation of phenylalanine hydroxylase. *Nat. Struct. Biol.* **1999**, *6*, 442−448.
(39) Martínez, A.; Knappskog, P. M.; Olafsdottir, S.; Døskeland, A. P.; Eiken, H. G.; et al. Expression of recombinant human phenylalanine hydroxylase as fusion protein in *Escherichia coli* circumvents proteolytic degradation by host cell proteases. Isolation and characterization of the wild-type enzyme. *Biochem. J.* **1995**, *306*, 589−597.
(40) Haavik, J.; Le Bourdelles, B.; Martínez, A.; Flatmark, T.; Mallet, J. Recombinant human tyrosine hydroxylase isozymes. Reconstitution with iron and inhibitory effect of other metal ions. *Eur. J. Biochem.* **1991**, *199*, 371−378.
(41) Meng, E. C.; Shoichet, B. K.; Kuntz, I. D. Automated docking with grid-based energy evaluation. *J. Comput. Chem.* **1992**, *13*, 505−524.
(42) Guex, N.; Peitsch, M. C. SWISS-MODEL and the Swiss-Pdb Viewer: an environment for comparative protein modeling. *Electrophoresis* **1997**, *18*, 2714−2723.
(43) Goodford, P. J. A computational procedure for determining energetically favorable binding sites on biologically important macromolecules. *J. Med. Chem.* **1985**, *28*, 849−857.
(44) Hubbard, S. J.; Campbell, S. F.; Thornton, J. M. Molecular recognition. Conformational analysis of limited proteolytic sites and serine proteinase protein inhibitors. *J. Mol. Biol.* **1991**, *220*, 507−530.
(45) Pey, A. L.; Thórólfsson, M.; Teigen, K.; Ugarte, M.; Martínez, A. Thermodynamic characterization of the binding of tetrahydropterins to phenylalanine hydroxylase. *J. Am. Chem. Soc.*, in press.
(46) Flatmark, T.; Almås, B.; Knappskog, P. M.; Berge, S. V.; Svebak, R. M.; et al. Tyrosine hydroxylase binds tetrahydrobiopterin cofactor with negative cooperativity, as shown by kinetic analyses and surface plasmon resonance detection. *Eur. J. Biochem.* **1999**, *262*, 840−849.
(47) Mayer, B.; Wu, C.; Gorren, A. C.; Pfeiffer, S.; Schmidt, K.; et al. Tetrahydrobiopterin binding to macrophage inducible nitric oxide synthase: heme spin shift and dimer stabilization by the potent pterin antagonist 4-amino-tetrahydrobiopterin. *Biochemistry* **1997**, *36*, 8422−8427.
(48) Gorren, A. C. F.; List, B. M.; Schrammel, A.; Pitters, E.; Hemmens, B.; et al. Tetrahydrobiopterin-free neuronal nitric oxide synthase: Evidence for two identical highly anticooperative pteridine binding sites. *Biochemistry* **1996**, *35*, 16735−16745.
(49) Wuthrich, K.; Billeter, M.; Braun, W. Pseudo-structures for the 20 common amino acids for use in studies of protein conformations by measurements of intramolecular proton−proton distance constraints with nuclear magnetic resonance. *J. Mol. Biol.* **1983**, *169*, 949−961.
(50) Gans, J. D.; Shalloway, D. Qmol: a program for molecular visualization on Windows-based PCs. *J. Mol. Graphics Modell.* **2001**, *19*, 557−559, 609.

JM0497646